

Characterizing Fabrication Process Induced Effects in Deep Submicron PHEMT's Using Spectrally Resolved Light Emission Imaging

Zhuyi Wang, Weidong Cai, Mengwei Zhang and G.P. Li

Department of Electrical and Computer Engineering

University of California, Irvine, 92697

E-mail: zhuyi@ece.uci.edu, Tel: (949) 824-4019, Fax: (949) 824-3732

Tony Hwang, Shyh-liang Fu, Patrick Chye, Kevin Schuerman and Sushila Venkatesan

Hewlett Packard Co., Santa Clara, CA 95054-3292 © 1999 GaAs Mantech

Abstract— Spectrally resolved light emission imaging technique was used for the first time in characterizing fabrication process variation induced effects on deep submicron power PHEMT's electrical characteristics. It is observed in devices processed with different conditions that the difference in gate leakage current can be attributed to gate misalignment as revealed both by emission imaging technique and scanning electron microscope. Defects in the active channel region were also located using the emission imaging technique. The defects have a characteristic of generation-recombination centers with a discrete energy level rendering the Lorentzian shape in drain current flicker noise spectrum.

Introduction

Recently, deep-submicron pseudomorphic GaAs HEMT's have shown superior power performance at microwave and millimeter wave frequencies. In order to develop a robust manufacturing technology and to realize fully the potential of the high performance power PHEMT technology, processing induced effects on device performance and reliability need to be properly addressed.

Although electrical testing (DC and RF) has been established for screening the processed PHEMT's wafers, these electrical specifications can not reveal the information of processing induced effects on devices. Furthermore, the non-uniform electric field and current distributions inside power PHEMT's can not be probed directly using the traditional electrical testing methods. The hidden device failures induced by high current density or high electric field spots can not be screened out. Thus a non-destructive inspection tool capable of identifying manufacturing process variation induced effects on device performance and of visualizing the electric field and current distribution inside the device is the most essential tool to assist engineers in further improving the manufacturing process control. An in-depth understanding of processing sensitivity on device design can also be comprehended.

In this paper, a novel technique, spectrally resolved electroluminescence imaging is developed to answer this challenge. With this technique, the distribution of current density and electric field inside device can be visualized for the first time.

Experimental

In order to deliver narrow band monochromatic images of high spatial resolution, a specially designed system has been developed (Fig. 1). It consists of three blocks. A

probe station with microscope is used to collect light emission from device under operation. A total magnification up to 1,000 times can be achieved in this system. An Acousto-Optic Tunable Filter (AOTF) is incorporated to provide a narrow band pass filtering function. The selected wavelength is ranged from 450nm to 1,100nm with 3-5nm spectral resolution. The third part is a LN₂ cooled high spatial resolution scientific CCD camera. The complete setup is computer controlled, fully automatic, suitable for on wafer or in package level testing.

The devices under investigation are multifinger power PHEMT's which have a gate length of 0.15 μ m and a source/drain spacing of 3 μ m with the gate being at the center of S/D. PHEMT's have a heavily uniform doped AlGaAs layer grown on top of InGaAs channel. Devices from two different processing conditions were used in this study.

Results and Discussions

(I) Spectrum and Mechanisms

Light emission is commonly observed from PHEMT's under normal operating condition. According to Wang *et al* [1], Zappe [2] and Zanoni *et al* [3], there are two dominant mechanisms responsible for light emission here. Bound state to bound state recombination inside InGaAs channel contributes to light emission at about 1 μ m wavelength and bremsstrahlung effect inside heavily doped AlGaAs layer contributes to light emission at shorter wavelength.

The typical emission spectrum from power PHEMT's is illustrated in Fig. 2. The sharp peak at 1 μ m due to a direct recombination and the Maxwellian distributed hot-carrier tail due to bremsstrahlung effect are evident in the graph. Comparing with the light emission spectrum from another PHEMT's [1] having a δ -doping profile in AlGaAs layer and biased at almost the same condition as ours, a much flatter hot carrier tail was observed in our current device. This suggests that a much higher electric field or electron temperature inside conducting channel in our device be accounted for the difference [3]. Since higher electric field is always expected in a heavily planar doped device than in a δ -doped one under the same bias condition, this hot carrier tail result is consistent with the different device structure used in our experiment.

(II) Gate Misalignment to Source/Drain

Power PHEMT's are often layouted in multifingers in order to deliver higher output power. Non-uniformity between different fingers will pose a potential threat to device reliability. Some fingers are more vulnerable to device breakdown while others are still left intact. Although non-

uniformity problems can originate from the starting substrate-epi wafer materials, they are more likely developed during fabrication processes such as mask alignment, recess etching and gate definition, etc.

The devices tested in our experiment are 4 finger PHEMT's manufactured under two different processing conditions. Fig. 3 illustrates their typical electrical characteristics. Although these devices showed a minor variation in drain current, their gate currents are distinctly different. Device from process #1 has a much lower peak gate current than that of #2. The gate current peaks at a more positive gate voltage in #1 than #2. The off-state leakage current at $V_{gs}=-0.5V$ shows a higher leakage level in device from process #2.

In order to understand what caused the difference, light emission images at two different wavelengths were taken on device biased at $V_{ds}=5V$ and $V_{gs}=0.4V$. The wavelength of $1\mu m$ and $0.63\mu m$, which are dominated by bound state to bound state recombination and bremsstrahlung effect respectively [1] are chosen here. Fig. 4 plots device #1's light intensity distributions among 4 fingers at $1\mu m$ and $0.63\mu m$ wavelength respectively. Not only are inhomogeneous distributions among 4 fingers observed, but they also show opposite patterns. Namely, finger #1 and #3 are brighter at $1\mu m$ wavelength than finger #2 and #4 while the latter two fingers are much brighter at $0.63\mu m$ wavelength than the former two.

According to Wang *et al* [1], light intensity at $1\mu m$ is proportional to the product of gate and drain current while light intensity at $0.63\mu m$ is proportional to gate current solely. Following this correlation and lucky electron model [4] [5], we can extract the relative distribution of both current (Fig.5a) and maximum channel electric field (Fig.5b) among 4 fingers. In these two plots, finger #1 and #3 actually have higher current density, while other two fingers have higher electric field. These results suggest that finger #1 and #3 have lower source resistance due to a shorter gate to source spacing, and that finger #2 and #4 have higher lateral electric field due to a shorter gate to drain spacing.

To confirm aforementioned hypothesis, the cross section of this device was studied by SEM as shown in Fig. 6a and 6b. Gate misalignments to source/drain are clearly seen. Each gate has about 30% offset to left-hand side. This means gate #1 and #3 are closer to source side while gate #2 and #4 are closer to drain side. This misalignment results in finger #1 and #3 having higher current while finger #2 and #4 having higher electric field under the same bias condition. This is consistent with the results obtained in Fig. 5a and 5b using the emission imaging technique. In contrast, Fig. 7a shows the light emission image from device #2. The light intensity distributions among 4 fingers are relatively uniform, suggesting no misalignment in this device. This was also confirmed by the SEM cross section of this device, illustrating gates sat at the center of S/D spacing (Fig. 7b).

The difference in the device cross section between device #1 and #2 may be responsible for their different gate current value in Fig. 3. It is worthwhile mentioning again that the gate leakage current is determined both by drain current and maximum electric field [4] [5]. Since the distributions of current and maximum electric field do not overlap with each other in device #1, its gate current is drastically lower than that of device #2 at more positive gate voltage. At the most negative gate voltage where device is biased under an off-state

condition, gate current should be solely determined by channel electric field. However, device #2 still has much higher gate current in this operating condition. We attribute this to their different surface property. Device #2 might have a non-ideal surface passivation, which acts as an additional source of gate leakage current.

(III) Dark Spots and Defects

Inhomogeneous light emission distribution along finger is very common and rather device dependent. This would project any physical irregularities along finger such as the one induced by defects in substrate-epi materials. Figure 8a shows light emission image at $1\mu m$ wavelength overlaying with its layout. Dark line spots were found on the rightmost finger. Since light emission at $1\mu m$ is attributed to carrier recombination inside InGaAs channel, any defects in the active region could act as non-radiative recombination centers. These generation and recombination centers typically have a discrete energy state inside the bandgap which might cause drain current low frequency flicker noise spectrum to deviate from ideal $1/f$ distribution.[6] The flicker noise spectrum taken from the same device is depicted in Fig. 8b, where a hump is clearly seen. On the other hand, the noise spectrum taken from the device shown in Fig. 7a illustrates an almost ideal $1/f$ shape (in dashed line).

Conclusions

A novel technique, spectrally resolved light emission imaging has been developed for the first time to characterize process variation induced effects on deep submicron power PHEMT's. Non-uniform distributions of current and electric field among 4 fingers have been visualized, consistent with SEM device cross section showing gate misalignment. Defects inside device were also detected using the image technique. The defects are confirmed in the measurement of drain current flicker noise spectrum. These new results suggest that the proposed non-invasive, 2-D inspection technique pose a great potential in real time, in-line device screening application for GaAs microwave/millimeter wave communication technology. It may also facilitate an in-depth study of the dependence of device performance on its structure and profile, leading to further optimization in device design.

Reference

- [1]Wang Z Y, *et al.*, "Deep submicron PHEMT's characterization with spectrally resolved carrier recombination imaging", 1998 IEDM Digest of Papers, pp. 239-242.
- [2]Zappe H P " Hot-electron electroluminescence in GaAs transistors", *Semicond. Sci. Technol.* 7, 1992, pp. 391-400.
- [3]Zanoli E, *et al.*, "Impact ionization and light emission in AlGaAs/GaAs HEMT's", *IEEE Transactions on Electron Devices*, vol.39, no. 8, Aug. 1992, pp. 1849-1856.
- [4]Hu C, *et al.*, "Hot -electron-induced MOSFET degradation-model, monitor and improvement", *IEEE Transactions on Electron Devices*, vol. ED-32, no.2, Feb. 1985, pp. 375-384.
- [5]Tam S, *et al.*, "Lucky-electron model of channel hot electron injection in MOSFET's", *IEEE Transactions on Electron Devices*, vol. ED-31, no. 9, Sept. 1984, pp. 1116-1125.
- [6]Ali F and Gupta A, "HEMT's and HBT's: Devices, fabrication, and Circuits", Artech House, 1991.

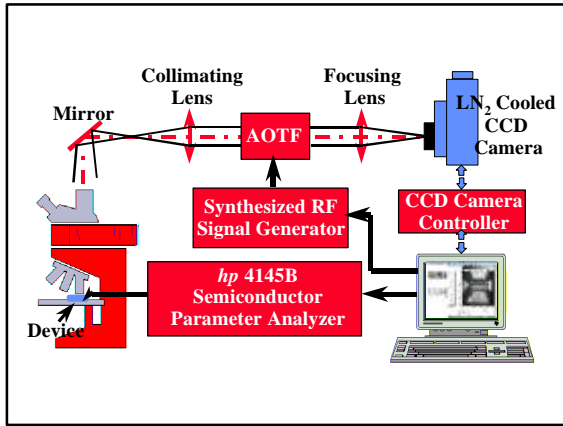


Fig. 1 Spectrally Resolved Imaging System

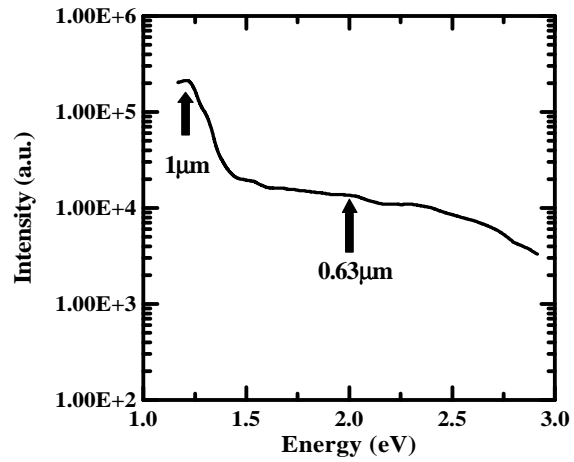


Fig. 2 Typical Spectrum of Light Emission from Power PHEMT

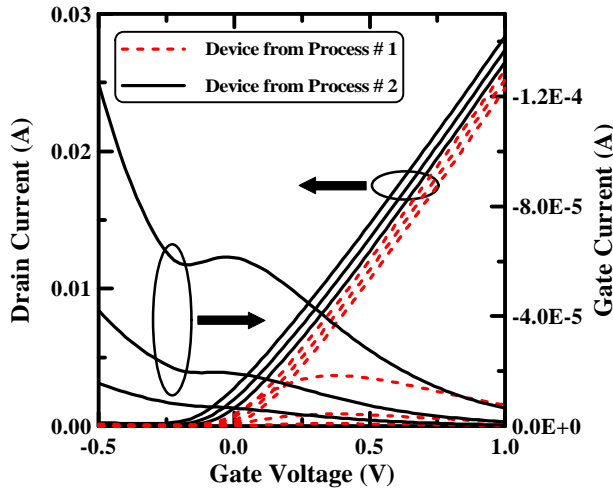


Fig. 3 Electrical Characteristics of PHEMT's from Two Processing Conditions

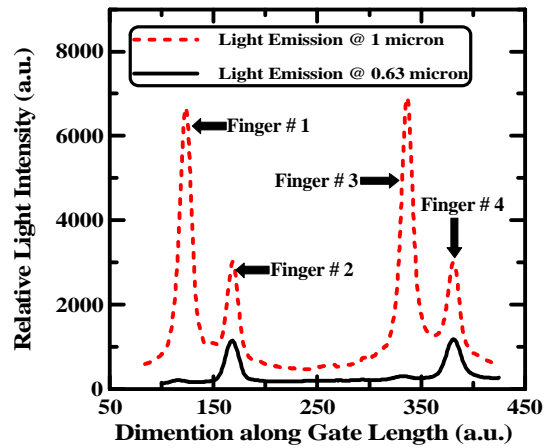


Fig. 4 Inhomogeneous Distribution of Light Intensity among 4 Fingers Showing Different Patterns at Different Wavelengths from Device of Process # 1

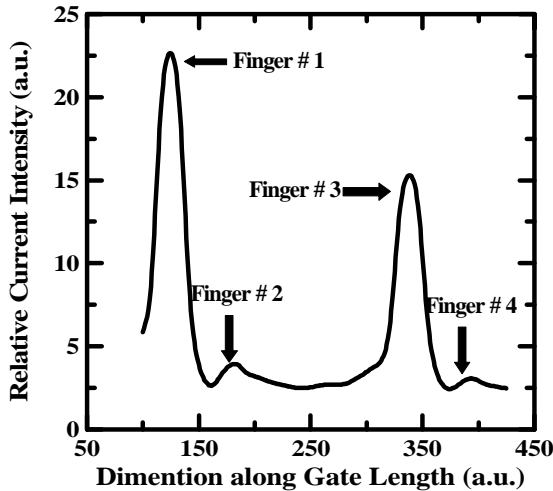


Fig. 5a Relative Channel Current Distribution among 4 Fingers

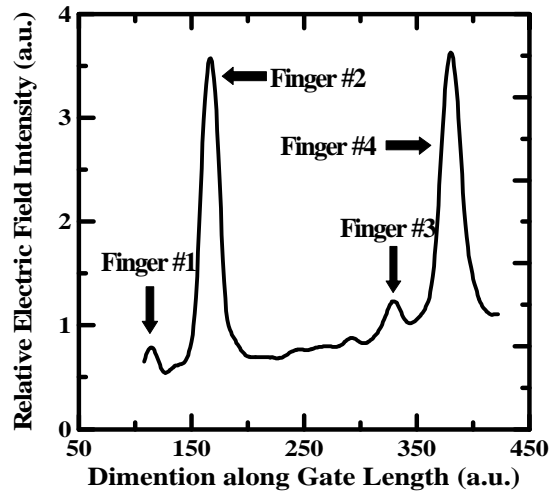


Fig. 5b Relative Maximum Electric Field Distribution among 4 Fingers

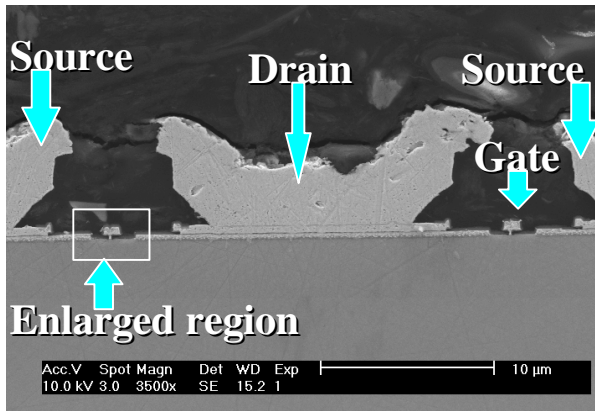


Fig. 6a SEM Cross Section of Device from Process # 1

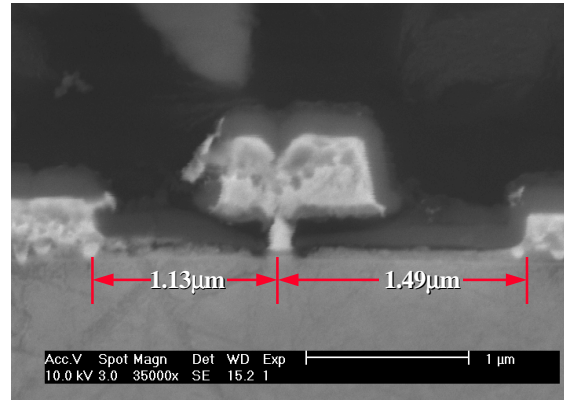


Fig. 6b Gate Misalignment of Device from Process # 1

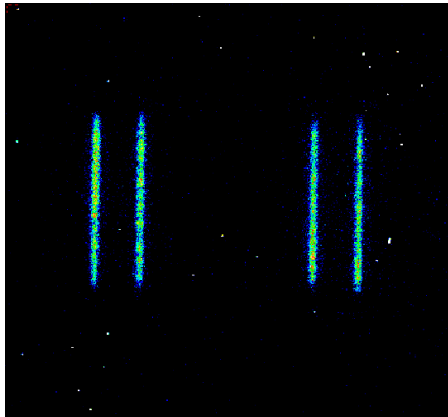


Fig. 7a Relatively Uniform Light Emission Distribution among 4 Fingers of Device from Process # 2

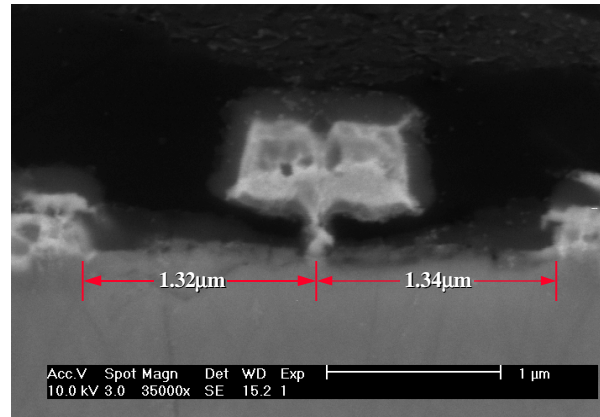


Fig. 7b No Gate Misalignment Found in Device from Process # 2

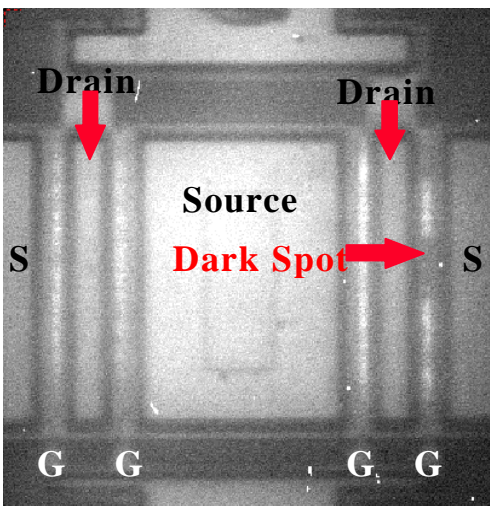


Fig. 8a Dark Spots of Light Emission at 1μm Found on One Finger

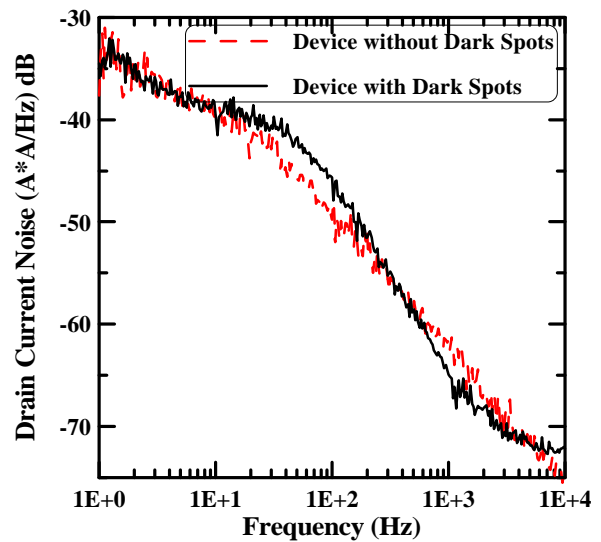


Fig. 8b Drain Current Flicker Noise Spectrum of Two Devices with and without Dark Spots

